Proceeding of the IEEE
International Conference on Robotics and Biomimetics
Dali, China, December 2019

A Legged Device Based on Active Buffering for Probe Landing on Micro-gravitational Asteroid*

Canhui Yin and Yilin Shen
State Key Laboratory of Robotics and System
Harbin Institute of Technology
Harbin, Heilongjiang Province, China
canhuiyin@163.com

Xiaolin Zhang
Beijing Institute of Spacecraft System Engineering
Beijing, China

Fan Guo
China Academy of space technology
Beijing, China

Qiquan Quan, Dewei Tang and Zongquan Deng
State Key Laboratory of Robotics and System
Harbin Institute of Technology
Harbin, Heilongjiang Province, China
quanqiquan@hit.edu.cn

***Abstract* -The landing of the probe on the asteroid surface provides the technical basis for in-situ exploration and sampling return and promotes to maximize the value of the probe. The micro-gravitation and the uncertainty in topography and geology on the asteroid surface pose challenges to the landing of the probe. To develop the asteroid landing technology, the legged landing device of asteroid probe based on active buffering mode is studied in this paper. The landing device adopts a three-legged structure to possess higher adaptability to the surface topography of asteroids and get the light and simple configuration. Besides, a buffering unit is designed based on the active mode of the damping motor which has obvious advantages in self-adaptability and autonomy. Through the comparison of various schemes, the slider-legged landing device is determined and designed in detail. On this basis, the co-simulation of the probe landing on the asteroid surface is completed, which shows the satisfaction of this device to reliability and efficiency. Finally, a prototype of the landing device is constructed and the micro-gravitational simulated test platform is developed to implement the landing buffering test of asteroid probe. The test results validate the performance of the landing device.**

Index Terms - Asteroid Exploration, Landing Device, Legged Structure, Damping Motor, Active Buffer.

I. INTRODUCTION

Asteroids are formed synchronously with the solar system and retain the materials of the early solar system. The severe meteorite impacts mainly caused by asteroids promoted the evolution of the Earth, and the impact threat of the near-Earth asteroids persists. Thus, asteroids have important exploration value of science, engineering, and commerce. Since the 1990s, advances in space technology have promoted the successive formation and development of various asteroid exploration methods, which include flying over, orbiting, impact, in-situ exploration, and sampling return. There are currently 11 deep space exploration missions for asteroids. The United States occupies the most missions [1][2][3][4][5][6][7]. Japan, ESA, and China also have some achievements [8][9][10]. In-situ exploration and sampling return are the only way to actively obtain mineralogical information of asteroids, and there are the higher technical difficulties. Landing on the asteroids can provide the necessary technical basis for in-situ exploration and sampling return. The operation makes the probe touch the asteroids surface safely and stay for a long time to realize the zero-distance study and promote the formation of the stable experimental platform on the asteroid surface, thus it greatly promotes to maximize the value of the probe. When the probe has the ability of multiple landing, it can detect many areas and it is also an important technical guarantee for the human landing on asteroids in the future.

In the current deep space exploration missions for the asteroids, some probes contacted with the asteroids and released small devices to the surface. This behaviors are defined as the generalized landing on asteroids. Probes getting the landing technology include NEAR, OSIRIS-Rex, Hayabusa and Hayabusa-2. The landing of NEAR on 433 Eros was an extended mission, and the probe had no landing device and corresponding descent strategy [11]. The ground control center used attitude control thrusters to brake the probe four times based on open-loop control strategy during the descent [12]. Once the probe contacted the surface, the thrusters produced counter-thrust to restrain the probe from bouncing and the probe panels embedding honeycomb aluminum absorbed part of the impact energy [13]. OSIRIS-Rex plans to contact 101955 Bennu surface for about 5 s under the Touch-And-Go (TAG) mode via a sampling device consisting of a three-joint manipulator and a disc sampling head at its end [14][15]. It buffers the impact by a compressible spring on the manipulator and obtains the adaptive capability to terrain via the universal joint connecting the manipulator and the disc sampling head [16]. Hayabusa also used the TAG mode, which made short contact with 25143 Itokawa for less than 1 s via a cylindrical sample

* This work is partially supported by NSFC Grant #51975139 to Q. Q. Quan and the Programme of Introducing Talents of Discipline to Universities ("111" Project) Grant #B07018.

978-1-7281-6321-5/19//$31.00 ©2019 IEEE

collector protruding from the abdomen. The sample collector had the middle section of weaving cylinder made of flexible materials which could make buffering [17][18]. Hayabusa also successfully deployed Target Marker (TM) with a diameter of about 0.1 m to the surface for optical navigation during descent. The TM was covered with a soft cloth filled with small high polymeric beads which had a low elastic recovery coefficient under micro-gravitational field [19]. Besides, Hayabusa also carried a 591 g surface jumping robot which was equipped with protruding needle-like rods to weaken the impact of landing. Hayabusa-2 inherited the TAG technology of Hayabusa. Besides, it carried a 9.6 kg small lander [20], which possessed the three-layer sandwich frame consisting of two light carbon-fiber-reinforced plastic sheets and a foam core. The frame could absorb part of the landing impact [21].

In this paper, a landing device of the asteroid probe is studied based on the micro-gravitation and uncertainty on the asteroid surface. Firstly, the scheme comparison and structural design of the landing device are implemented. Then, the simulation of the landing buffering of the asteroid probe is completed. Further, the prototype of the landing device and the micro-gravitational simulation platform are constructed, and the landing buffering test of asteroid probe is carried out. Finally, the conclusion is presented.

II. Schemes Comparison and Structural Design of Landing Device

The landing device of asteroid probe mainly includes the landing support structure and impact buffering unit. The support structure supports and stabilizes the main probe body. This structure is designed in the legged-type, which has higher adaptability to terrain gradient and fluctuation compared with the continuous structures such as the ring. The three-legged structure is suitable for landing of small size and light-load probes with the lightest and simplest configuration. Due to the micro-gravitation on the asteroid surface and the low initial landing velocity of the probe, the three-legged structure is chosen as the landing support. The impact buffering unit absorbs the impact energy during landing to ensure that the probe does not overturn or escape. The micro-gravitation and the uncertainty in topography and geology on the asteroid surface make the probe have a strong tendency to roll continuously and even escape due to the bounce, and it is sensitive to small external excitation. Thus, the impact buffering unit should have high adaptability and autonomy. Active buffering uses controlled and adjustable buffering units to absorb landing impact energy. Compared with passive buffering based on honeycomb aluminum, metal spring and hydraulic damping, the active buffering has more obvious advantages in adaptability and autonomy. Moreover, the micro-gravitation on asteroids makes the dynamic process on its surface have the equivalent slow-velocity attribute, which also provides favorable conditions for the application of active buffering mode. Therefore, the active buffering mode based on damping motor is adopted in impacting buffering unit. This also enables the device to have the ability to repeat landing.

A. Comparative Analysis of Various Legged Schemes

Based on the active buffering mode of damping motor, three schemes of landing device are designed as slider-legged, swing-legged and four-linkage-legged (FL-legged). They all consisted of three same landing legs which are evenly fixed at the outer edge of the probe main body, as shown in Fig. 1(a). The leg of the slider-legged device is composed of the fixed leg bar (FLB), movable leg bar (MLB), rope-pulley mechanism (RPM), and damping motor unit (DMU), as shown in Fig. 1(b). The movable leg bar is installed inside of the fixed leg bar and can slide along their common axis. The fixed leg bar is fixed to the bottom of the probe main body. The rope-pulley mechanism and the damping motor unit are combined to connect two leg bar to form an interrelated whole. When the probe lands on the asteroid surface, the moving leg bar slides upwards along its axis relative to the fixed leg bar at a certain distance under the action of the surface contact force. The slide is converted and amplified into the rotation of the motor shaft by the rope-pulley mechanism and the reducer inside the damping motor unit. Thus, the landing impact energy is transformed into internal energy for dissipation. Each landing leg of the swing-legged device is mounted on the probe through a rotary joint and the damping motor unit is located at this rotary joint, as shown in Fig. 1(c). The leg will swing when its end touches the asteroid surface and drive the motor to rotate via the reducer. In the four-linkage-legged landing device, landing leg has the four-linkage structure, and its base is the probe main body, as is shown in Fig. 1(d). The damping motor unit is arranged in the upper base joint (joint a) of four-linkage structure to make this joint active, while the others are passive.

According to the overall design requirements of the asteroid probe, the mass of the probe is m, and its bottom has a width of D and a height of H to the ground. When the landing legs are in the initial configuration condition, the connecting line from the sole to the root of landing legs forms an angle of θ with the horizontal line. According to the control accuracy, the probe remains the initial landing velocity of v related to the normal direction of the asteroid surface. Besides, it is subject to the counter-thrust force P along its normal direction to point to the surface. When the probe lands, the landing leg bears the normal reaction force of F from the surface. Make F=150 N based on the characteristics of a soft landing. Consider the extreme landing situation, that is, only a single leg develops the effective buffering. For the slider-legged landing device, L is the straight buffering stroke of the

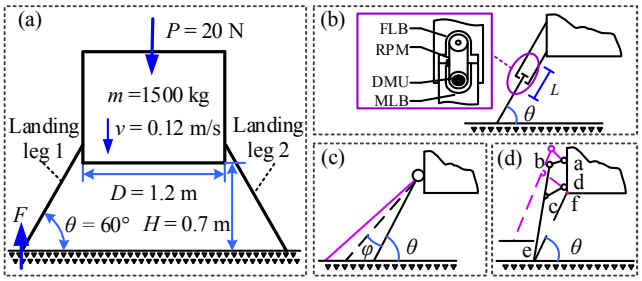

Fig. 1 Schematic diagram of three-legged landing devices

leg, and T_r and φ are the output moment and output angle of the reducer respectively, and R is the radius of the pulley. Assuming that the main body decelerates uniformly after the probe contacts the surface during the landing buffering, the smaller the pulley radius R is, the smaller the output torque T_r of the reducer is. If R=10 mm, then (1) can be obtained.

$$\begin{aligned} &L = 95.92\,\text{mm} \\ &T_r \cdot \varphi = 12.46\,\text{J} \;\Rightarrow T_r = 1.3\,\text{N}\cdot\text{m},\ \varphi = 9.58\,\text{rad} = 549^\circ \end{aligned} \tag{1}$$

For the swing-legged landing device, extreme landing conditions are also considered and other constraints remain unchanged. Then (2) is obtained, in which h is the descending height of the main body of the probe during landing.

$$\begin{aligned} &\varphi = \arccos((H-h)/(H/\sin(\pi/3))) - \pi/6 = 10.24^\circ \\ &T_{\text{r-min}} = FH\tan(\pi/6) = 60.62\,\text{N}\cdot\text{m} \\ &T_{\text{r-max}} = F(H-h)\tan(\pi/6 + 0.241) = 78.32\,\text{N}\cdot\text{m} \end{aligned} \tag{2}$$

For a four-linkage-legged landing device, (3) can be obtained based on the extreme landing conditions.

$$\begin{aligned} \frac{T_r}{F} = {} & L_{\text{cf}}\sin(\angle\text{cdf} - \angle\text{bcd}) + L_{\text{cd}}\sin\angle\text{cdf} \\ & - \frac{L_{\text{be}}\sin(\angle\text{cdf} - \angle\text{bcd})}{L_{\text{bc}}\sin\angle\text{bcd}} L_{\text{ad}}\sin\angle\text{cdf} \end{aligned} \tag{3}$$

The reasonable size of the landing leg is determined as shown in (4).

$$\begin{aligned} &L_{\text{ad}} = 200\,\text{mm},\ L_{\text{ab}} = 180\,\text{mm},\ L_{\text{bc}} = 180\,\text{mm} \\ &L_{\text{cd}} = 200\,\text{mm},\ L_{\text{ce}} = 723\,\text{mm},\ L_{\text{df}} = 100\,\text{mm} \end{aligned} \tag{4}$$

Substituting (4) into (3) to obtain (5), where $T_{\text{r-s}}$ is the initial output moment of the reducer and $T_{\text{r-e}}$ is the end output moment of the reducer.

$$\begin{aligned} &\angle\text{bad}_{\text{-min}} = 33.76^\circ,\ (\angle\text{cdf} - \angle\text{bcd})_{\text{-max}} = 19.68^\circ \\ &\Rightarrow T_{\text{r-s}} = -6.4\,\text{N}\cdot\text{m} \\ &\angle\text{bad}_{\text{-max}} = 83.54^\circ,\ (\angle\text{cdf} - \angle\text{bcd})_{\text{-min}} = 6.74^\circ \\ &\Rightarrow T_{\text{r-e}} = 24.96\,\text{N}\cdot\text{m} \\ &\varphi = \angle\text{bad}_{\text{-max}} - \angle\text{bad}_{\text{-min}} = 49.78^\circ \end{aligned} \tag{5}$$

According to the above design, the main performance parameters of each scheme are obtained as shown in Table I. It can be seen that the descending height of the probe main body is same when three landing devices work under the same total energy absorption condition. During buffering, the lateral retraction distance of a single leg of the sliding-legged landing device is less than 50% of both that of the other two landing devices. Besides, the lateral retraction of the single leg of the sliding-legged landing device is to close inwards, which reduces the size requirement to flat landing area to lower the difficulty of landing site selection. Meanwhile, the buffering torque required by slider-legged landing device is much less than both that of the other two landing device. It reduces the requirement and quality of motor and deceleration components, and it is advantageous to improve the landing stability because the damping torque keeps unchanged during the buffering process. Thus, the slider-legged landing device has obvious advantages over the swing-legged and the four-linkage-legged landing device and it is determined to be used for the landing buffering of the probe on the asteroid surface.

TABLE I
PARAMETERS OF THREE-LEGGED LANDING DEVICE IN MULTIPLE SCENARIOS

Parameter	Slider-legged	Swing-legged	FL-legged
Descent height	83 mm	83 mm	83 mm
Sliding distance	47.96 mm	118 mm	119.23 mm
Damping torque	1.3 N·m	60.62~78.32 N·m	0~24.96 N·m
Buffering stroke	95.92 mm	10.24°	49.76°

B. *Structural design*

Detailed structural design of the slider-legged landing device is completed and the single leg is shown in Fig. 2. The landing leg consists of the pedestal, fixed leg bar, movable leg bar, footpad, rope-pulley mechanism, and damping motor unit. The damping motor unit absorbs the main landing impact energy and sliding friction between two leg bars makes auxiliary buffering. The fixed leg bar is fixed with the pedestal. The relative sliding distance of two leg bars is in the range of 0~110 mm, that is, the maximum landing buffering stroke is 110 mm. The disc footpad is installed at the bottom of the movable leg bar via the ball-hinge pair. The rope-pulley mechanism is composed of the T-shaped frame, wire clip, driving pulley, transmission rope, tensioner pulley, driven pulley, connecting block, and bracket. The damping motor unit mainly includes a motor, reducer and bevel gear set. The braking torque of the motor is transmitted to the driving pulley through the reducer and bevel gear set. The motor, reducer, bevel gear set, and driving pulley are installed on the outer surface of the fixed leg bar through the T-shaped frame. To realize this function that the braking torque on the driving pulley is transferred to the moveable leg bar, the transmission rope is clamped by the connecting block to fixed with the movable leg bar and it is wound around the driven pulley to form a transmission loop. The driven pulley is mounted on the outer surface of the fixed leg bar through a bracket. To ensure that the transmission rope does not jump on the driving pulley, a wire clip and a tensioner pulley are set to tighten the rope.

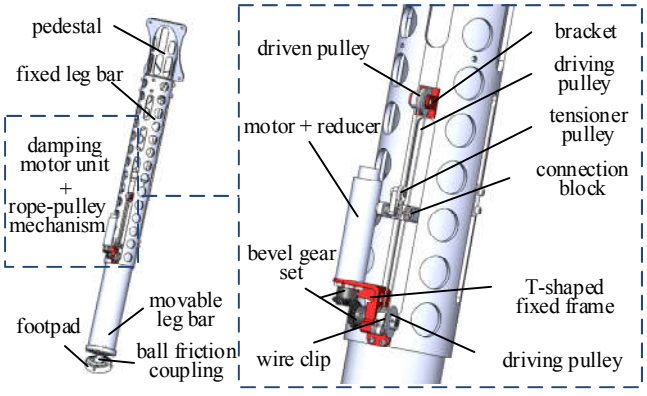

Fig. 2 Structural design of a single leg of the landing device

III. Co-simulation of Landing Buffering

The ADAMS and MATLAB are employed to simulate the probe landing on the asteroid surface under the PID strategy of the damping motor. Due to the unknown environment feature on the asteroid, its surface is set to rigid to consider the unfavorable buffering situations. The simulation parameters are set as shown in Table II, which include the probe mass m, gravity acceleration g, initial vertical landing velocity v_v and horizontal velocity v_h, counter-thrust force P, surface friction coefficient μ, surface contact damping C and stiffness K. The dynamic co-simulation aiming at the reliability and efficiency of the landing device is carried out under the situations of single-legged and three-legged landing buffering respectively.

A. *Vertical single-legged landing buffering*

In the simulation of single-legged landing buffering, the landing device model is simplified to eliminate the influence of ineffective landing legs. Here, the probe is equipped with one landing leg fixed at the center of the bottom of the probe main body and its main axis coincides with the normal of the probe, as shown in Fig. 3. Due to landing with a single leg, the initial landing horizontal velocity is not considered, that is, v_h=0 m/s, and the probe has no attitude dip angle. Through simulation, the displacement d_p, velocity v_p and acceleration a_p of the probe main body, the damping torque T_D of the damping motor unit, and the contact force F between the landing leg and asteroid surface are obtained, as shown in Fig. 4. With the PID strategy,

TABLE II
PARAMETERS SETTING OF LANDING SIMULATION

Parameter	Value	Parameter	Value
m	1500 kg	P	20
g	0	μ	0.6
v_v	0.12 m/s	C	10 N·s/mm
v_h	0.05 m/s	K	1×10^5 N/mm

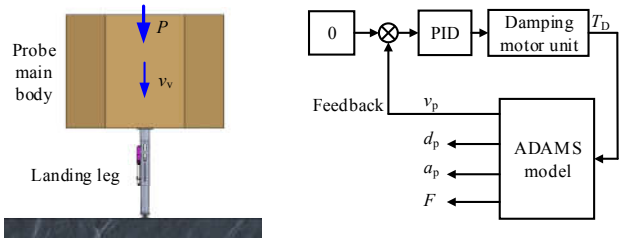

Fig. 3 Co-simulation model of single-legged landing buffering

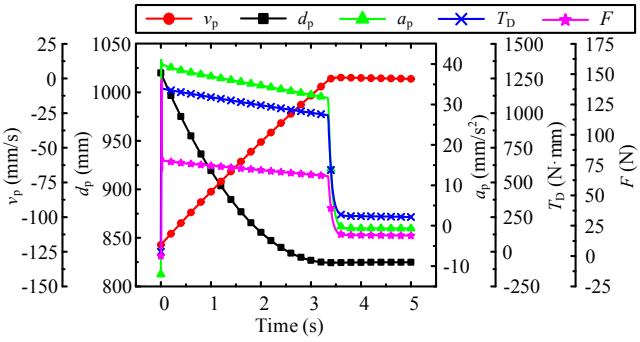

Fig. 4 Simulation results of single-legged landing buffering

the velocity of the probe decreases to 0 m/s at 3.4 s when it is stable on the asteroid surface, as shown in Fig. 4. Then the motor only provides the torque to keep the position of the probe main body unchanged. The probe did not bounce during the landing process, and the maximum contact force between the leg and the surface is F_{max}=146 N which occurs at the initial contact moment. There is the contact force F<100 N in the subsequent landing buffering process. According to the result, the landing device can achieve the safe soft landing of the probe on the asteroid surface and satisfy the reliability requirements under the unfavorable landing situations.

B. *Three-legged landing buffering*

Three-legged landing buffering is the expected working mode, so its co-simulation is completed to measure the efficiency of the landing device. Here, three landing legs are uniformly distributed on the outer edge of the bottom of the probe. Besides, the probe has no attitude dip angle. The initial horizontal landing velocity is considered. The displacement and velocity of the probe main body in the vertical direction during landing are obtained via simulating, as shown in Fig. 5. The output torques of the damping motor unit and the contact forces between the legs and the surface are shown in Fig. 6. According to the results, the velocity of the probe decreases to 0 m/s at 0.88 s when the probe is stable on the surface. Then the motors only provide the torques to hold the probe main body. Fig. 6 shows that the probe did not bounce and the maximum contact force is F_{max}=200 N. The contact force fluctuated slightly during the process but has the value of F<116 N. The fluctuation is mainly caused by the initial horizontal landing velocity which also caused the differences in damping torques and contact forces on each leg shown in Fig. 6. In summary, the landing device can quickly consume the impact energy and then maintain the attitude stability of the probe in the case of three-legged landing buffering, so that it satisfies the requirements of high efficiency.

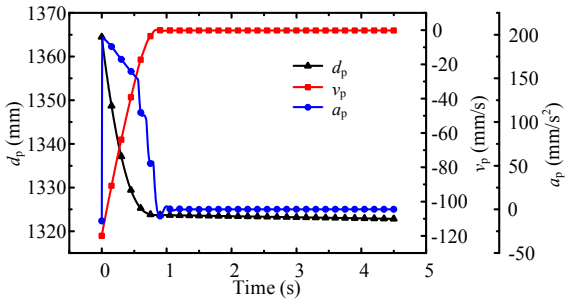

Fig. 5 Simulation results of three-legged landing buffering

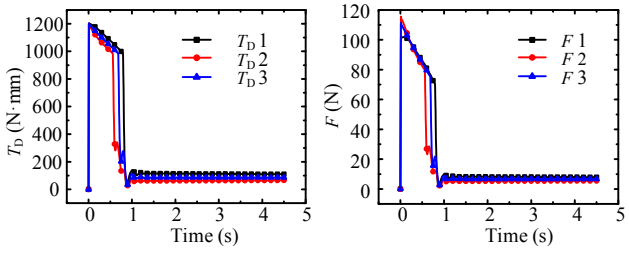

Fig. 6 Damping torque and contact force of each landing leg

IV. Prototype Development and Landing Test Study

A. Landing device prototype and test platform

The prototype of the landing device is built according to Fig. 2. The test platform for landing buffering of the probe is developed the verification. This platform consists of the simulated probe main body (SPMB), cold gas thrust system (CGTS), motion state generator, and reconfigurable simulated asteroid surface (RSAS). The simulated probe main body adopts the frame structure filled with the mass blocks to get the changeable mass. The cold gas thrust system provides the landing counter-thrust force P which remains unchanged in a single test. The motion state generator counteracts the gravity of the probe and impose the two-dimensional initial landing velocity on it. This part mainly consists of the normal moving platform (NMP), tangential moving platform (TMP), turntable, counterweight components (CC), and pedestal. In each moving platform, a servo motor drives slide-rail pair through pulley transmissions to provide the probe with two moving degrees of freedom (TY, TZ) in the horizontal plane to obtain the initial horizontal velocity v_h (+Y) and vertical velocity v_v (+Z) related to the simulated asteroid surface. The turntable is located on the upper layer of the two moving platforms and enables the probe to have a certain degree of rotational freedom (RX) around the vertical direction. The counterweight components are matched with two moving platforms to balance the frictions on the two slide-rail pairs. The pedestal is the base of the motion state generator. The simulated surface can be embedded with different materials to simulate various asteroid surfaces.

For the above parts, the landing leg is fixed at the simulated probe main body which is installed on the turntable, and the reconfigurable simulated asteroid surface is placed vertically in front of the probe. The prototypes of the landing device and the test platform and their installation relationship are all shown in Fig. 7. In the tests, the motor of the moving platform will generate the initial landing velocity for the probe after being started. Once the velocity reaches the requirement, the motor stops and the slide-rail pair is disconnected from the pulley transmission to make the probe move freely on the guide rail. A pressure sensor is installed on the footpad to obtain the contact force between the probe and the simulated surface. It is used for landing triggering and recording the landing contact force. When the landing triggers, the motor on the landing leg turns into the controlled damping mode to consume the impact energy and the cold gas thrust system starts to provide counter-thrust force for the probe.

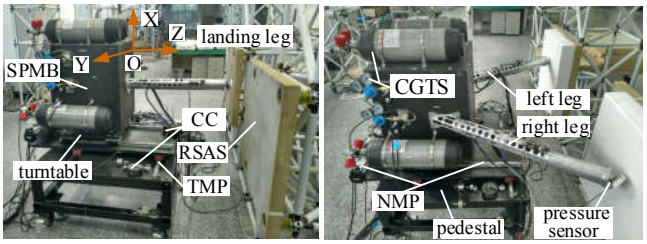

(a) (b)

Fig. 7 Prototypes of landing device and test platform

B. Principle verification tests and result analysis

The landing tests of probe equipped with a vertical single leg is achieved to verify the ultimate buffering capacity of the damping motor unit, as shown in Fig. 7 (a). The material of the footpad is aluminum. The mass of the probe main body is two-thirds of the actual mass, that is, m=1000 kg. The cold gas thrust system generates the force of 20 N. The motion state generator provides the probe with a vertical initial velocity of +0.1 m/s via the normal moving platform, while the tangential moving platform and the turntable are locked. The simulated surface uses two materials which are sandstone (SS) and foam board (FB). The sandstone represents the rigid and hard media to test the impact energy dissipation features of the landing leg. The foam board represents soft media to simulate the thick regolith. Several tests have been carried out with two kinds of materials and the results of the same material have a good consistency. A result under each material is chosen, then the peak current I_{max} of the damping motor unit, contact force F between footpad and surface, the duration t of probe achieving stabilization, buffering stroke L of the landing leg, and buffering effect are shown in Table III. The change of contact force F with time under each material is shown in Fig. 8.

When the probe lands on the sandstone, the footpad keeps in touch with sandstone all the time after contacting with it, and there is no bounce. When it comes to the foam board, the footpad bounced slightly once after contacting and then the probe stabilized quickly with the counter-thrust force. In two groups of tests, the peak value of the pressure sensor is less than 300 N, and the landing leg achieves buffering within 3 s with the total buffering stroke less than 100 mm. So the tests prove that the landing leg has a reliable buffering ability.

The landing tests of probe equipped with two legs installed symmetrically is completed to test the adaptability and efficiency of the buffering mode and the structure of landing device, as shown in Fig. 7 (b). There is the counter-thrust force of 10 N and the motion state generator provides the probe with the initial vertical velocity of +0.1 m/s and horizontal velocity of +0.05 m/s. Here, the turntable is released. To discuss the influence of different contact friction, the footpads of aluminium (Al) and polytetrafluoroethylene

TABLE III
Test Results of Vertical Single Leg Landing

Surface	I_{max} (A)	F_{max} (N)	t (s)	L (mm)	Effect
SS	2.367	289	2	98	N[a]
FB	2.367	300	3	90	Y[b]

[a]N represents No bounce. [b]Y represents Buffering successfully after bounce.

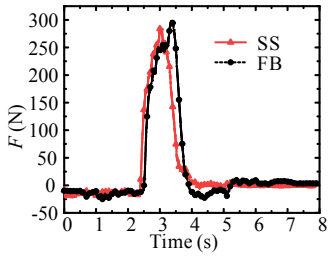

Fig. 8 Contact force curves of single-legged buffering test

TABLE IV
TEST RESULTS OF LANDING WITH TWO LEGS INSTALLED SYMMETRICALLY

Surface	F (N)		t (s)	L (mm)		Footpad	Effect
	LL	RL		LL	RL		
SS	221	271	1.5	15	7	Al	N
	258	330	2	6	1	PTFE	Y
FB	279	276	2.5	1	1	Al	Y
	300	304	2	2	1	PTFE	Y

(PTEF) are employed to produce high and low friction coefficient respectively. Four groups of tests are produced under the different combination of footpad materials and simulated surface. The test results in each group are in good agreement. A result of each group test is chosen and shown in Table IV. For the plantar contact force and the buffering stroke of the landing leg, there are two parts respectively corresponding to the left leg (LL) and the right leg (RL).

The test results show that the footpads keep in touch with the simulated surface and do not bounce only when the material of the footpads are aluminium and the probe lands on sandstone. In other cases, the footpads all bounce slightly after contacting with the simulated surface and then it can stabilize quickly. It shows that it will be disadvantageous to the safe berthing and attitude stability of the probe when the landing contact stiffness and the friction coefficient are small under the current buffering control strategy. The peak value of pressure sensor is less than 330 N and the landing legs achieve buffering within 2.5 s in the four groups of tests. In the tests, the buffering strokes of the landing legs are small and the internal sliding frictions between the landing leg bars play the major buffering role. Therefore, the above tests validate the adaptability and efficiency of the landing device.

V. CONCLUSION

In this paper, a landing device for asteroid probe is studied. It enables the probe to land safely and stably on the asteroid surface with the features of micro-gravitation and uncertainty. Besides, it has the ability of repeatable landing. The landing device has three sliding bar legs adapting to the terrain gradient and fluctuation well. A damping motor unit is arranged on each landing leg to consume landing impact energy of the probe based on the active buffering mode. The internal linear movement of the sliding bar leg is transformed into the rotation of the damping motor shaft by the rope-pulley mechanism, which contributes to eliminate the larger impact at the initial landing contact moment by its own flexibility. On the basis of the detailed structure of the landing device, the landing buffering co-simulations of the probe are completed, which show that the landing device satisfies the requirements of reliability and efficiency well. Furthermore, a prototype of landing device is constructed and a micro-gravitational simulation platform is developed to carry out the landing tests of asteroid probe. The test results validate the performance of the landing device. In the future, the control strategy of the damping motor with high robustness and the distribution of dissipation of landing impact energy will be researched.

REFERENCES

[1] M. J. S. Belton, et al, "Galileo encounter with 951 Gaspra: First pictures of an asteroid," *Science*, vol. 257, no. 5077, pp. 1647–1652, 1992.

[2] M. J. Belton, et al, "Galileo's encounter with 243 Ida: An overview of the imaging experiment," *Icarus*, vol. 120, no. 1, pp. 1–19, 1996.

[3] J. Veverka, et al, "NEAR encounter with asteroid 253 Mathilde: overview," *Icarus*, vol. 140, no. 1, pp. 3–16,1999.

[4] J. Oberst, et al, "A model for rotation and shape of asteroid 9969 Braille from ground-based observations and images obtained during the Deep Space 1 (DS1) flyby," *Icarus*, vol. 153, no. 1, pp. 16–23, 2001.

[5] T. C. Duxbury, et al, "Asteroid 5535 Annefrank size, shape, and orientation: Stardust first results," *Journal of Geophysical Research: Planets*, vol. 109, no. E2, 2004.

[6] C. Tubiana, R. Duffard, L. Barrera, and H. Boehnhardt, "Photometric and spectroscopic observations of (132524) 2002 JF56: fly-by target of the New Horizons mission," *Astronomy and Astrophysics*, vol. 463, no. 3, pp. 1197–1199, 2007.

[7] A. S. Konopliv, et al, "The Vesta gravity field, spin pole and rotation period, landmark positions, and ephemeris from the Dawn tracking and optical data," *Icarus*, vol. 240, pp. 103-117, 2014.

[8] A. Accomazzo, K. R. Wirth, S. Lodiot, M. Kuppers, and G. Schwehm, "The flyby of Rosetta at asteroid Šteins–mission and science operations," *Planetary and Space Science*, vol. 58, no. 9, pp. 1058–1065, 2010.

[9] R. Schulz, H. Sierks, M. Küppers, and A. Accomazzo, "Rosetta fly-by at asteroid (21) Lutetia: An overview," *Planetary and Space Science*, vol. 66, no. 1, pp. 2–8, 2012.

[10] J. C. Huang, et al, "The Ginger-shaped Asteroid 4179 Toutatis: New Observations from a Successful Flyby of Chang'e-2," *Scientific reports*, vol. 3, no. 1, 2013.

[11] D. W. Dunham, et al, "Implementation of the first asteroid landing," *Icarus*, vol. 159, no. 2, pp. 433–438, 2002.

[12] L. Prockter, et al, "The NEAR shoemaker mission to asteroid 433 eros," *Acta Astronautica*, vol. 51, no. 1-9, pp. 491–500, 2002.

[13] J. Veverka, et al, "The landing of the NEAR-Shoemaker spacecraft on asteroid 433 Eros," *Nature*, vol. 413, no. 6854, pp. 390–393, 2001.

[14] D. S. Lauretta, et al, "OSIRIS-REx: sample return from asteroid (101955) Bennu," *Space Science Reviews*, vol. 212, no. 1-2, pp.925–984, 2017.

[15] A. May, et al, "OSIRIS-REx touch-and-go (TAG) mission design for asteroid sample collection". *In 65th International Astronautical Congress*, 2014.

[16] E. B. Bierhaus, et al, "The OSIRIS-REx spacecraft and the touch-and-go sample acquisition mechanism (TAGSAM)," *Space Science Reviews*, vol. 214, no. 7, pp. 107, 2018.

[17] J. I. Kawaguchi, K. Uesugi, and A. Fujiwara, "The MUSES-C mission for the sample and return—its technology development status and readiness," *Acta Astronautica*, vol. 52, no. 2-6, pp. 117–123, 2003.

[18] T. Kubota, M. Otsuki, and T. Hashimoto, "Touchdown dynamics for sample collection in Hayabusa mission," *In 2008 IEEE International Conference on Robotics and Automation*. IEEE, pp. 158–163, 2008.

[19] T. Kubota, S. Sawai, T. Hashimoto, and J. Kawaguchi, "Robotics and autonomous technology for asteroid sample return mission," *In ICAR'05. Proceedings., 12th International Conference on Advanced Robotics*. IEEE, pp. 31–38, 2005.

[20] Y. Tsuda, M. Yoshikawa, T. Saiki, S. Nakazawa, and S. Watanabe, "Hayabusa2–Sample return and kinetic impact mission to near-earth asteroid Ryugu". *Acta Astronautica*, vol. 156, pp. 387–393, 2019.

[21] T. M. Ho, et al, "MASCOT—the mobile asteroid surface scout onboard the HAYABUSA2 mission," *Space Science Reviews*, vol. 208, no. 1-4, pp. 339–374, 2017.